

ULTRASOUND INTERACTIVE SEGMENTATION WITH TENSOR-GRAPH METHODS

Nicola Rieke* Christoph Hennemersperger* Diana Mateus*[†] Nassir Navab*

* Chair of Computer Aided Medical Procedures, Technische Universität München, Germany.

[†] Institute for Computational Biology, Helmholtz Zentrum München, Germany

ABSTRACT

We address the problem of segmenting aortic aneurysms in ultrasound images. As solution we propose a novel framework based on graph-based interactive segmentation methods, such as graph-cuts and random walks. Our main contribution is extending these approaches to handle structure tensor ultrasound images. Our hypothesis is that the structure tensor is better suited to represent the contextual information in ultrasound images than the pure b-mode intensity values. We demonstrate that this extension significantly improves the performance of both methods in clinical data.

1. INTRODUCTION

Ultrasound imaging plays a crucial role in diagnosis of cardiovascular diseases. One major application is here the examination of the abdominal aorta, where it is of interest for vascular surgeons to detect malformations like aneurysms (AAA). Volume and shape of these aneurysms determine strong risk indicators for rupture [1]. Nevertheless, these parameters are not used in today’s clinical practice due to the lack of methods to accurately delineate these structures.

Despite recent advances, fully automatic segmentation in ultrasound images is still challenging, mainly due to ultrasound physical properties (echo, shadow, reflexions, etc.) that degrade image quality and make the recognition of edges difficult [2]. In recent years, these challenges have been addressed in different ways [3], *e.g.* improving edge responses, including learning and prior knowledge, or with the help of semi-automatic methods. In this work, we are interested in *graph-based* approaches, as they allow for an easy interaction, provide global optimal solutions and are a good alternative to the sensitivity of contour-based methods to both the initialisation and spurious edges.

One of the most successful graph-based algorithms for semi-automatic segmentation is *graph-cuts* [4]. More recently, Grady [5] proposed the *random walker* approach, which combines a simplified formulation of the problem and an efficient solution, while it does not suffer from the small-cut problem. In the context of ultrasound image segmentation, graph-based approaches still have problems when directly applied to intensity images, mainly due to the weak

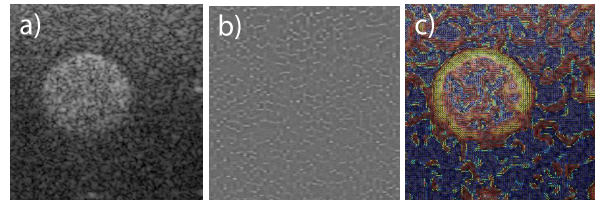


Fig. 1. Gradient vs. structure tensor. a) original US image, b) gradient magnitude, c) structure tensors shown as ellipses and colour indicating the magnitude of the largest eigenvalue.

and noisy edge responses. One way to overcome such problems is to consider the context of each pixel instead of the intensities alone. Prior work in this direction has considered the use of texture features [6] and modeling the spatial correlation of speckle [7]. Instead, we characterise the context of a pixel in terms of its *structure tensor*, which serves especially well in inferring structure from sparse and noisy data [8], facilitating the distinction between regions with different structure (*c.f.* Fig 1). Our contribution is an ultrasound graph-based segmentation method that integrates the image tensor representation. The difficulty lies in the definition of adequate graph weights, as conventionally these are associated to pairwise node (dis)similarities and computed on the basis of an Euclidean norm. As structure tensors do not form a vector-space, it is required to consider (dis)similarities that account the Riemannian nature of the tensor space [9]. Segmentation methods using tensors and Riemannian metrics have been proposed for graph-cuts approaches [10, 11], but in medical imaging they have been applied exclusively to Diffusion Tensor Images (DTI) [12]. In the case of the random walker, the extension to tensor images was only recently explored in [13] also in the context of DTI. To the best of our knowledge, modelling ultrasound images with structure tensors and extending graph-cuts and random walker algorithms to handle them, is a novel approach to ultrasound image segmentation.

A quantitative evaluation of the proposed framework, called hereafter *Tensor-graph (TG)*, is performed on 40 patient datasets with highly-developed abdominal aortic aneurysms in clinical diagnosis. We show that the dice similarity coefficient as well local curvature deviation determining smoothness of the segmentation results are better using TG compared to classical intensity-based approaches.

2. METHOD

Consider a scalar valued ultrasound image $I : \Omega \subset \mathbb{R} \rightarrow \mathbb{R}, p \mapsto I(p)$. The segmentation problem consists in partitioning the image into two disjoint sets, *i.e.* $I = O \cup B$, where O and B are sets of pixels representing the object and background, respectively. In an interactive framework, the user defines the hard constraints by selecting pixels serving as seeds for object and background. The proposed Tensor Graph (TG) approach is an interactive method consisting of three parts: i) seed selection; ii) computation of the structure tensor images; and iii) graph-based segmentation method. We start by describing the computation of the structure tensor image. Then, we recall the two standard graph-based segmentation methods: graph-cuts or random walker. Finally, we explain how to define proper edge weights in order to apply the graph segmentation methods to tensor images.

2.1. Structure tensor image

Ultrasound images are noisy and do not provide clear edges on the boundaries of objects. Therefore, segmentation methods relying on gradients are prone to fail. Our idea is to use additional texture information by computing the 2D structure tensor \mathbf{T} for every pixel $p \in \Omega$:

$$\mathbf{T}(p) = \begin{pmatrix} G * I_x(p)^2 & G * I_x(p) I_y(p) \\ G * I_x(p) I_y(p) & G * I_y(p)^2 \end{pmatrix} \quad (1)$$

where G is a Gaussian smoothing kernel and $I_x(p)$ and $I_y(p)$ are the partial derivatives of the scalar valued image I at pixel p . The resulting tensor image is $I_T : \Omega \subset \mathbb{R} \rightarrow S_+^2, p \mapsto \mathbf{T}(p)$, where there is a symmetric and semi-positive definite 2x2 matrix for every pixel in I . The usage of this second moment matrix provides two advantages: first, the distribution of the noisy intensity values of the ultrasound image is smoothed, which improves the segmentation robustness. Second, the predominant directions of the gradient are captured providing texture information. Thus, we use I_T instead of I as input to the graph-based segmentation algorithm.

2.2. Graph-based methods

Let the image be modelled as an undirected graph $G = (V, E)$ with vertex set V and edge set E , where each node in V stands for a pixel and every edge e_{ij} connecting nodes $v_i, v_j \in V$ is assigned a weight w_{ij} . Also assume that seed points for object (S_O) and background (S_B) are given. The segmentation problem can then be cast to a binary graph partitioning. Next, we briefly recall the graph-cuts and random walker partitioning criteria and solution.

Graph cuts: Here, edges connecting neighbouring nodes ($e_{ij} \in E$) are called *n-links* and express their similarity. Two terminal nodes are added to the graph: the sink node b representing the background and the source node o representing the object. Every non-terminal node $v \in V$ is connected

to the terminal nodes via edges called *t-links*, expressing the likelihood of v belonging to the object or background region respectively. We denote the corresponding edge weights with w_p^n and w_p^t , for n-links and t-links respectively. Graph cuts looks for the *minimal cut* separating the vertex set V into two disjoint sets O and B , where $o \in O$ and $b \in B$. Formally, the minimised energy is:

$$F(\mathbf{A}) = \sum_{p \in I} w_p^t(A_p) + \lambda \sum_{(p,q) \in N, A_p \neq A_q} w_p^n(p, q) \quad (2)$$

where N are all unordered neighbourhood pixel pairs, λ is a balancing parameter, and \mathbf{A} is the set of current pixel assignments A_p to the object or background region. For more details on the solution of the graph-cuts problem and an efficient solution, we point the reader to [4].

Random walker: Introduced by Grady [5], the random walker method does not require additional nodes. Here, the edge weights are interpreted as the likelihood that a random walker crosses an edge. The ensemble of seeds belonging both to object and background are denoted with $S = S_O \cup S_B$, and all other pixels form the set \bar{S} , so that $V = S \cup \bar{S}$. To assign $v_i \in \bar{S}$ to one region, we compute the probability x_i^s that a random walker starting from v_i will first reach a seed point $s \in S$. Then, the pixel is assigned to the region containing the seed point with the highest probability. Let \mathbf{L} be the Graph-Laplacian:

$$\mathbf{L}_{ij} = \begin{cases} \sum w_{ij}, & \text{if } i = j \\ -w_{ij} & \text{if } v_i \text{ and } v_j \text{ are adjacent nodes} \\ 0, & \text{otherwise} \end{cases} \quad (3)$$

Then, the algorithm optimises the energy $F(\mathbf{x}^s) = \mathbf{x}^{s\top} \mathbf{L} \mathbf{x}^s$. For seed nodes, the constraints $x_i = 1 \forall v_i \in S_O$ and $x_i = 0 \forall v_i \in S_B$ are imposed. A solution is found by decomposing \mathbf{L} according to marked (\mathbf{L}_M) and unmarked (\mathbf{L}_U) nodes $\mathbf{L} = \begin{pmatrix} \mathbf{L}_M & \mathbf{B} \\ \mathbf{B}^T & \mathbf{L}_U \end{pmatrix}$, and solving the linear system (see [5] for more details):

$$\mathbf{L}_U \mathbf{x}^s = -\mathbf{B}^T \mathbf{m}^s, \text{ with } m_j^s = \begin{cases} 1, & \text{if } v_j \in S \\ 0 & \text{if } v_j \in \bar{S} \end{cases}$$

2.3. Determining the edge weights

The crucial part in both methods is the definition of the edge weights. Since tensors do not form a vector space, a dissimilarity measure between the nodes has to respect the conical structure of the tensor space, while assigning small values only to tensors of the same structure. A distance fulfilling these requirements is the Information Geodesic Distance [12]:

$$\begin{aligned} d(\mathbf{T}_i, \mathbf{T}_j) &= \sqrt{\frac{1}{2} \text{tr} \left(\log^2 \left(\mathbf{T}_i^{-\frac{1}{2}} \mathbf{T}_j \mathbf{T}_i^{-\frac{1}{2}} \right) \right)} & (4) \\ &= \sqrt{\frac{1}{2} \sum_{i=1}^m \log^2(\phi_i)} & (5) \end{aligned}$$

where $\text{tr}(\cdot)$ denotes the trace of the matrix, \log the matrix logarithm and ϕ_i are the m eigenvalues of the determinantal equation $|\phi \mathbf{T}_j - \mathbf{T}_i| = 0$. This distance satisfies the properties of a metric on a Riemannian manifold and offers the advantage of being an intrinsic distance measure. Using $d(\mathbf{T}_i, \mathbf{T}_j)$, we determine the edge weights needed for the two graph-based segmentation methods.

Graph cuts weights: In order to fulfil that the user selected pixels are correctly assigned to source and sink, the corresponding t-links are set to the lower (0) and upper limits M , respectively. We compute M following [14]. All other t-weights from node v_i to a terminal node are computed as the distance of \mathbf{T}_i to the mean tensor of the respective seed set:

$$w_{ij}^t = \lambda \cdot d(\mathbf{T}_i, \text{mean}(S)), \quad \text{mean}(S) = \sum_{\mathbf{T}_l \in S} \frac{\mathbf{T}_l}{|S|}$$

where $S = Bg \wedge Ob$ and $j = b \wedge o$. The weights for the n-links are computed via the dissimilarity measure d defined in Eq 4. A summary of the edge weights is given in table 1.

Table 1. Edge weights for Graph Cut Algorithm

Edge	Link	For	Weight
$(\mathbf{T}_i, \mathbf{T}_j)$	n-link	$\mathbf{T}_i, \mathbf{T}_j \in V, i \neq j$	$d(\mathbf{T}_i, \mathbf{T}_j)$
(\mathbf{T}_i, s)	t-link to source	$\mathbf{T}_i \notin S_O \cup S_B$	$\lambda \cdot d(\mathbf{T}_i, \text{mean}(S_B))$
		$\mathbf{T}_i \in S_O$	M
	$\mathbf{T}_i \in S_B$	0	
(\mathbf{T}_i, t)	t-link to sink	$\mathbf{T}_i \notin S_O \cup S_B$	$\lambda \cdot d(\mathbf{T}_i, \text{mean}(S_O))$
		$\mathbf{T}_i \in S_O$	0
	$\mathbf{T}_i \in S_B$	M	

Random Walker weights: Originally the edge weight between two pixels is defined by a Gaussian weighting function of the difference of their intensity values. Since we are working in tensor space, we modified edge weights to

$$w_{ij} = \exp(-\beta \cdot d(\mathbf{T}_i, \mathbf{T}_j)^2) \quad (6)$$

where $d(\cdot, \cdot)$ is the dissimilarity measure defined in Eq 4 and β is the only free parameter.

3. EXPERIMENTAL VALIDATION

We validated all methods on datasets obtained with a Curefab CS 3D US system connected to a GE Logic 7 ultrasound scanner. Ultrasound b-mode scans of abdominal aortic aneurysms (AAA) from routine diagnostics as well as pre- and post-operative sets were acquired clinically for 20 patients by a trained physician. For every patient, two frames located approximately at the maximum aneurysm diameter were selected and manually segmented for ground truth retrieval resulting in a total set of 40 ultrasound slices. We evaluated the two presented tensor-graph approaches in comparison to their classical counterparts based on intensity information. For estimation of the structure tensor and the smoothed intensities required for the intensity-based methods, a Gaussian

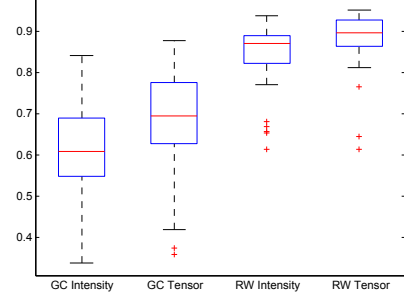


Fig. 2. dice similarity coefficients for all evaluated ultrasound images compared for graph cuts (GC) and random walks (RW) using tensor and intensity information.

kernel width should be selected according to the object-boundary widths. We evaluated various widths in the range from $0.5mm$ to $16mm$ and chose for our experiments a window size of $8mm$ as this gave the overall best results for aortic images. Parameter $\lambda = 0.1$ was fixed similar to [10] for the graph-cuts, while $\beta = 90$ was set to provide robust segmentations for the random-walks [5]. For both methods, we used a 4-connectivity neighborhood and manually selected object seed points once per image.

The overall similarity of our segmentation results to ground truth delineation was evaluated by means of the dice similarity coefficient. The results of all datasets are depicted in Fig 2 with median dice coefficients of 0.694 ± 0.12 and 0.896 ± 0.07 for the tensor-graph approaches using graph-cuts and random walks compared to 0.608 ± 0.11 and 0.870 ± 0.08 for the intensity based approaches respectively. Furthermore, a qualitative comparison of the four presented methods is shown in Fig 3 for one of the evaluated images. In terms of segmentation methods it can be observed that both graph-cuts approaches perform considerably worse compared to the random-walkers. The reason for this is the definition of the t-weights for the graph-cuts, which is based on the mean tensor of an object seed set. As ultrasound images in general contain speckle and appear heterogeneous also within anatomical objects, the usage of mean tensors is not adequate. The random walks methods which rely on local neighborhood information only, consistently provide higher dice scores.

By comparing intensity-based and tensor-graph methods, it is clearly shown that the overall dice scores improve for both tensor-graph methods compared to their classical counterparts. The benefit of tensor-graphs especially becomes clear by comparing the results for the random walks framework in Fig 3, where the tensor-based segmentation matches the ground-truth delineation accurately even in the regions where intensity border information is missing. It is also notably that the *intensity-based* random-walker method tends to produce unsteady contours with partial leakage. Although shape priors could improve the results, we avoid their use in favour of the generality of the method. The steadiness of segmentation results in ultrasound imaging is in general

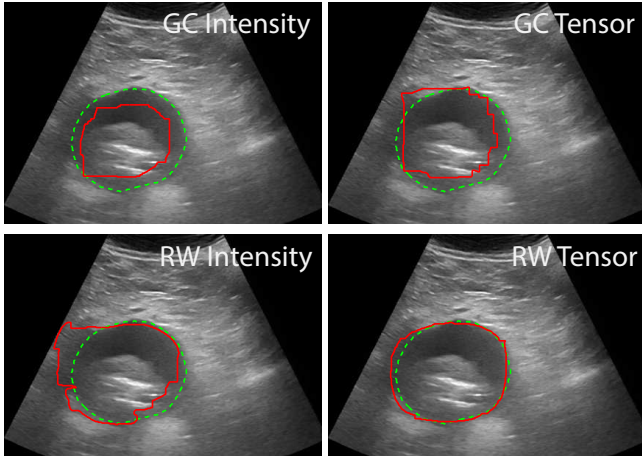


Fig. 3. Segmentation results for one ultrasound slice. Green dashed and red solid contours mark ground truth and segmentation result for the compared methods.

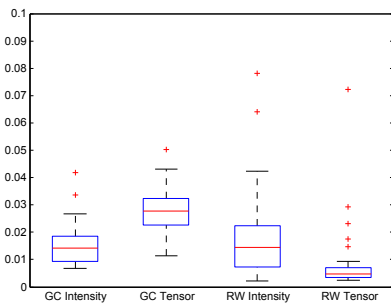


Fig. 4. Variance of local curvature for the compared methods.

challenging due to i) strong variations in local intensity values, and ii) partially missing borders because of different ultrasonic attenuation. Therefore, we also evaluated the deviation in local curvature of the segmented contours, measured as the variance of local contour curvature. Our results are shown in Fig 4 and confirm the qualitative impressions: both intensity-based methods are sensitive to local intensity variations, resulting in a frayed contour shape. Additionally, the graph-cuts methods suffer from the mean-tensor estimation, while the random-walks tensor-graph method provides smooth contours with the lowest overall variance.

4. CONCLUSION

We have presented a new interactive segmentation approach based on a tensor-graph representation for ultrasound imaging. We showed that local information computed via the structure tensor can be used to incorporate contextual information into segmentation, which leads to improved results compared to intensity-based approaches. One limitation of the current approach is the fixed neighbourhood size for tensor computation. An interesting direction for future work is a multi-scale extension, both to enable interactive segmentation without required prior knowledge and to handle

segmentations of structures at different scales.

5. REFERENCES

- [1] DA Vorp, ML Raghavan, and MW Webster, “Mechanical wall stress in abdominal aortic aneurysm: influence of diameter and asymmetry,” *Journal of Vascular Surgery*, vol. 27, no. 4, pp. 632–639, 1998.
- [2] A Noble and D Boukerroui, “Ultrasound image segmentation: a survey,” *TMI*, vol. 25, no. 8, 2006.
- [3] A Noble, “Ultrasound image segmentation and tissue characterization,” *Journal of Engineering in Medicine*, vol. 224, no. 2, pp. 307–316, February 2010.
- [4] Y Boykov and V Kolmogorov, “An experimental comparison of min-cut/max-flow algorithms for energy minimization in vision,” *TPAMI*, vol. 26, no. 9, 2004.
- [5] L Grady, “Random walks for image segmentation,” *TPAMI*, vol. 28, no. 11, pp. 1768–1783, Nov. 2006.
- [6] L Gupta, RS Sisodia, V Pallavi, C Firtion, and G Ramachandran, “Segmentation of 2D fetal ultrasound images by exploiting context information using conditional random fields,” in *EMBC*, 2011, pp. 7219–7222.
- [7] G Slabaugh, G Unal, T Fang, and M Wels, “Ultrasound-specific segmentation via decorrelation and statistical region-based active contours,” in *CVPR*, 2006.
- [8] MS Lee G. Medioni and CK Tang, *A Computational Framework for Feature Extraction and Segmentation*, Elsevier, 2000.
- [9] X Pennec, P Fillard, and N Ayache, “A Riemannian framework for tensor computing,” *IJCV*, vol. 66, pp. 41–66, 2006.
- [10] J Malcolm, Y Rathi, and A Tannenbaum, “A graph cut approach to image segmentation in tensor space,” in *CVPR*, 2007.
- [11] S Han, W Tao, D Wang, XC Tai, and X Wu, “Image segmentation based on grabcut framework integrating multiscale nonlinear structure tensor,” *TIP*, vol. 18, no. 10, pp. 2289–2302, 2009.
- [12] R Luis-García, C Alberola-López, and CF Westin, “On the choice of a tensor distance for DTI white matter segmentation,” in *New Developments in the Visualization and Processing of Tensor Fields*. Springer, 2012.
- [13] S El-Hilo, YT Weldeselassie, and MS Atkins, “Comparison between fourth and second order DT-MR image segmentations,” in *SPIE*, 2011.
- [14] YT Weldeselassie and G Hamarneh, “DT-MRI segmentation using graph cuts,” in *SPIE*, 2007, vol. 6512.